SEE-OFDM: Spectral and Energy Efficient OFDM for Optical IM/DD Systems*

H. Elgala and T.D.C. Little
Multimedia Communications Laboratory
Department of Electrical and Computer Engineering
Boston University, Boston, Massachusetts
{*helgala, tdcl*}*@bu.edu*

August 15, 2014

MCL Technical Report No. 08-15-2014

Abstract–In the next major phase of mobile telecommunications standards "5G," Visible Light Communication (VLC) technology or light fidelity (Li-Fi) has great potential to be a breakthrough technology in the future of wireless Internet access. We propose a novel real-valued unipolar version of orthogonal frequency division multiplexing (OFDM) that is suitable for direct intensity modulation with direct detection (IM/DD) optical wireless systems including VLC. Without additional forms of interference estimation and cancelation to recover the symbols, the Spectral and Energy Efficient OFDM (SEE-OFDM) almost doubles the spectral efficiency of unipolar optical OFDM formats. In our scheme, multiple signals are generated and added/transmitted together, where both odd and even indexed subcarriers of the inverse fast Fourier transform (IFFT) operation carry data and are not affected by any kind of interference, (*e.g.*, clipping). Monte Carlo simulations under additive white Gaussian noise (AWGN) show gains of up to 6dB in signal-to-noise ratio (SNR) compared to the conventional energy-efficient asymmetrically clipped optical OFDM (ACO-OFDM). Moreover, a peak-to-average power ratio (PAPR) reduction of 2.5dB is obtained as a bonus. Therefore, advantages such as increased data rate and reduced PAPR make the proposed SEE-OFDM very attractive for optical wireless systems.

Keywords: OFDM, IM/DD, VLC, Li-Fi, LEDs, Clipping.

*In *Proc. IEEE International Symposium on Personal, Indoor and Mobile Radio Communications (PIMRC 2014)*, September 2-5, 2014, Capital Hilton, Washington DC. This work is supported by the NSF under grant No. EEC-0812056. Any opinions, findings, and conclusions or recommendations expressed in this material are those of the author(s) and do not necessarily reflect the views of the National Science Foundation.

1 Introduction

The number of multimedia capable and Internet connected mobile devices is rapidly increasing. Ericsson envisions that there will be 50 billion connected devices by 2020 [1]. Watching HD streaming videos and accessing cloud-based services are the main user activities consuming data capacity in the future. The high demand for such massive data traffic that is expected to grow 10-fold by end of 2016 will drive the trend of using a wide range of spectrum [2]. The use of diverse spectrum includes the farther limits of radio spectrum to 300 GHz and beyond and including the use of the visible spectrum. In terms of network topology, heterogeneous networks (HetNets) will play an important role towards the goal of using a diverse spectrum to provide high quality of service, especially in indoor enviroments where there is localized infrastructure supporting short-range directional services. This is suppoted by data indicating that a majority of mobile traffic (70%) occurs indoors [2]. In future wireless cellular networks based on the Long Term Evolution (LTE) standard, signals of macro-cells will cover a large area while indoor small-cells (pico-cells or Wi-Fi access points) deployed under coverage of the macro-cells will take over the connection when moving indoors [3]. Such signals' coexistence forms two-layer wireless signal coverage typical of HetNets. Optical wireless communication (OWC) systems, and specifically based on the VLC technology, transmit data on the intensity of optical sources, usually via light emitting diodes (LEDs) [4]. VLC-enabled indoor luminaries and street lights can be modeled as small-cells in a HetNet where a three-layer network formed by RF macro-cells, RF pico-cells/Wi-Fi and Li-Fi (the most recent and used name for VLC networks) transmissions are deployed. The vision is that a Li-Fi wireless network would complement existing heterogenous RF wireless networks, and would provide significant spectrum relief by allowing mobile and Wi-Fi systems to off-load a significant portion of wireless data traffic [5].

The simplest and cost-effective way to realize VLC transmission is through direct IM/DD [6]. Targeting hundreds of Mbps, single-carrier modulation techniques such as on-off keying (OOK) and pulse-position modulation (PPM) suffer from inter-symbol interference (ISI) due to multipath propagation. In terms of transmitter electronics, a bandwidth-limited operation due to off-the-shelf LEDs' modulation bandwidth, limits the use of the single-carrier techniques towards 1Gbps. Hence, a multi-carrier technique based on orthogonal subcarriers carrying complex constellations and more resilient to multipath propagation such as OFDM is required. Further benefits of this modulation scheme include adaptive bit and power loading and simple equalization with single-tap equalizers in the frequency domain. From a networking perspective, OFDM offers a flexible multiple access implementation through orthogonal frequency division multiple access (OFDMA) that is also used in the LTE standard. Therefore, the application of OFDM in hybrid RF-optical mobile networks would allow the use of the already established higher level communication protocols used in LTE and the reuse of the baseband signal processing and resource management techniques.

For energy-efficient optical IM/DD systems that do not require DC biasing of the optical source, the baseband OFDM signal must be positive (*i.e.* real valued and unipolar). However, conventional OFDM signals are complex-valued and bipolar in nature. Therefore, the well-known RF-OFDM format has to be modified in order to become suitable for IM/DD systems [7, 8]. A straightforward way is to impose a Hermitian symmetry constraint in the frequency domain on the subcarriers of the IFFT operation. However, such DC-biased optical OFDM (DCO-OFDM) signal generated in the time-domain is still bipolar; DC bias is required for proper operation where the bipolar signal is su-

perimposed on this DC operating point. Significant efforts are devoted to designing optical OFDM formats which are purely unipolar. All well-known solutions that do not require interference estimation and cancelation at the receiver must sacrfice half the spectral efficiency, for example, data rates are halved as compared to DCO-OFDM. These solutions include the asymmetrically clipped optical OFDM (ACO-OFDM) [9] and Flip-OFDM [10].

We propose a novel optical OFDM format called SEE-OFDM to carry data on odd as well as even indexed subcarriers of the IFFT operation. The approach is based on generating multiple signals using only odd indexed subcarriers (similar to ACO-OFDM) using different IFFT lengths and simple signal construction/conditioning and reconstruction steps at the transmitter and the receiver, respectively. The maximum IFFT length is N. The generated signals using different paths (each IFFT operation is associated to a path) are added together before being transmitted. At a fixed average power per time-domain OFDM symbol, such signal summation leads to a desired reduction of the PAPR as the power is distributed among the different signals. At the transmitter, the signal construction/conditioning realizes the distribution of the subcarriers among both even and odd indexed subcarriers and insures the clipping of all negative signal values in order to maintain no DC-bias operation. The receiver requires a single Fast Fourier Transform (FFT) operation of length N. Simple reconstruction steps at the receiver achieve the elimination of the clipping interference. SEE-OFDM advantages include zero DC-bias, higher data rates and reduced PAPR while insuring minimal increase in computational complexity.

The paper is organized as follows. In Section II, the SEE-OFDM transmitter is introduced. The SEE-OFDM receiver is explained in Section III and Section IV presents the obtained simulation results. Finally, the conclusions are given in Section V.

2 The SEE-OFDM Transmitter

Assuming two-paths approach, the SEE-OFDM signal is the sum of two real-valued unipolar signals that are generated using two different paths. The building blocks of the SEE-OFDM transmitter is shown in Fig. 1. The first path "single-path" is almost a conventional ACO-OFDM transmission chain. The data is an input stream of grouped ones and zeros "bit-symbols" based on the considered quadrature amplitude modulation (QAM) or phase shift keying (PSK) constellations. The generated complex "QAM/PSK-symbols" are then mapped onto the following vector:

$$X_k = \left[\, 0\, X_0 \cdots \;\; 0 \;\; X_{N/4-1} \;\; 0\, X^*_{N/4-1} \;\; 0 \cdots \;\; X^*_0 \,\right]^T \tag{1}$$

where, $(.)^*$ denotes the complex conjugate, $(.)^T$ denotes the transpose of a vector and the values $X_k, k = 0, \cdots, N-1$ are the N frequency-domain input symbols. While mapping the QAM/PSK-symbols to only odd indexed subcarriers of the length N IFFT operation, the Hermitian symmetry property of the vector X is needed to insure real-valued output signal. The values of the first and the $N/2$ subcarriers must be also zero to ensure the Hermitian property. The time-domain output signal is generated by taking the IFFT of the vector X_k:

$$x_n = \frac{1}{N} \sum_{k=1}^{N} X_k \exp^{\left(j\frac{2\pi}{N}nk\right)} \tag{2}$$

where, $x_n, n = 0, \cdots, N-1$ are the N time-domain output samples. Since X_k contains data only on the odd subcarriers, the generated time-domain signal has a half-wave symmetry. The

half-wave symmetry means that the same information in the first $N/2$ samples is repeated in the second half of the OFDM symbol. As a consequence, the negative part can be clipped without any loss of information. This clipping produces a unipolar signal. The intermodulation caused by clipping occurs only in the even indexed subcarriers and does not affect the data-carrying odd indexed subcarriers.

As shown in Fig. 1, the same procedure is repeated in the second path using a length $N/2$ IFFT operation. Instead of signal clipping, the polarity of the -ve samples are flipped and horizontally concatenated with the +ve samples to form a length N time-domain OFDM symbol. Both signals after the construction/conditioning step(s) are summed and finally a cyclic prefix (CP) is added. The CP is needed to avoid inter-carrier interference (ICI) as well as inter-block interference (IBI) by converting the linear convolution with the channel into a circular one. The resulting unipolar time-domain signal, and after being converted to an analog signal through the digital-to-analog converter (D/A), is used to modulate the intensity of the LED.

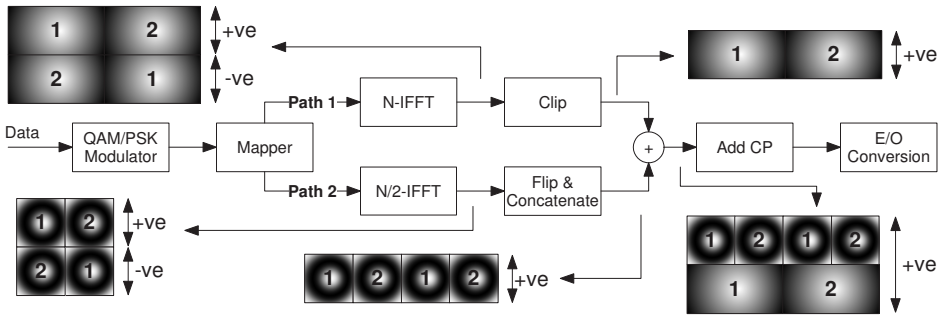

Figure 1: Two-paths SEE-OFDM transmitter.

Therefore, the achieved data rate for such two-paths SEE-OFDM system is given by,

$$\begin{aligned} R_{\text{total}} &= R_{\text{path 1}} + R_{\text{path 2}} \\ &= \left(\frac{(N/4)+(N/8)}{N+N_{\text{CP}}}\right) B \log_2 M \end{aligned} \tag{3}$$

where, B denotes the bandwidth, N_{CP} denotes the number of time-domain samples used in the CP, and M is the QAM/PSK modulation order.

3 The SEE-OFDM Receiver

The building blocks of the SEE-OFDM receiver is shown in Fig. 2. Signal reconstruction steps are required before applying a single length N FFT operation. The main purpose of the reconstruction is to eliminate the intermodulation caused by the signal clipping in the first path which occurs in the even indexed subcarriers used by the second path. Applying the FFT operation using the original bipolar signal of the first path will eliminate the clipping interference falling on the even indexed subcarriers.

How the signal of the second path is transmitting symbols on the even indexed subcarriers is now explained. The receiver decodes the time-domain OFDM symbol x_n by performing the FFT

operation,

$$X_k = \sum_{n=1}^{N} x_n \exp^{\left(-j\frac{2\pi}{N}nk\right)} \tag{4}$$

When the FFT is performed over two consecutive and identical OFDM symbols (see the signal symmetry from the second path in Fig. 1 and Fig. 2). The output of the FFT can be written as,

$$X_k = \sum_{n=1}^{N/2} x_n \exp^{\left(-j\frac{2\pi}{2N}nk\right)} + \sum_{n=N/2+1}^{N} x_n \exp^{\left(-j\frac{2\pi}{2N}nk\right)} \tag{5}$$

Since the first $N/2$ transmitted samples are identical to the last $N/2$ samples, (*i.e.*, $x_n = x_n + N/2$, for n = 1 to $N/2$), we can re-write the above equation as,

$$X_k = \sum_{n=1}^{N/2} x_n \exp^{\left(-j\frac{2\pi}{2N}nk\right)} + \sum_{n=1}^{N/2} x_n \exp^{\left(-j\frac{2\pi}{2N}(n+N/2)k\right)} \tag{6}$$

After simplification, we get:

$$X_k = \sum_{n=1}^{N} x_n \exp^{\left(-j\frac{2\pi}{2N}nk\right)} (1 + e^{\frac{-j\pi k}{2}}) \tag{7}$$

Now, when k is an even number, $(1 + e^{\frac{-j\pi k}{2}}) = 2$, but when k is an odd number, $(1 + e^{\frac{-j\pi k}{2}}) = 0$. Thus, the above equation can be re-written as,

$$X_{2l} = 2\sum_{n=1}^{N} x_n \exp^{\left(-j\frac{2\pi}{N}nk\right)} (1 + e^{\frac{-j\pi k}{2}}) \tag{8}$$

$$X_{2l+1} = 0 \tag{9}$$

where, X_{2l} are the even indexed subcarriers, X_{2l+1} are the odd indexed subcarriers and $l = 0, \cdots, N/2 - 1$. Thus, the odd indexed subcarriers are zero and the even indexed subcarriers capture the output of a length N FFT on a single OFDM symbol (Equ. (8)).

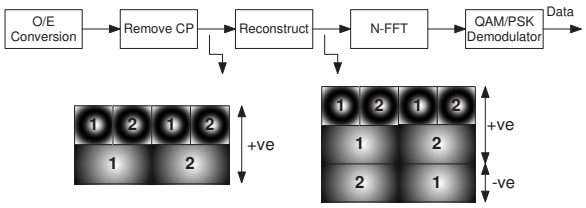

Figure 2: Two-paths SEE-OFDM receiver.

At the receiver, and after the optical-to-electrical conversion using an optical detector (photo-diode) and assuming an AWGN channel model, the time-domain samples can be expressed as follows:

$$y[n] = x[n] \otimes h[n] + z[n] \tag{10}$$

where, h[n] is the impulse response of the channel ($h[h] = \delta[n]$), $z[n]$ is the AWGN with variance σ_z^2 (*i.e.,* noise power and $\otimes$ denotes a convolution operation). As shown in Fig. 3, the first step in the reconstruction process is the substraction of the second half-period $y_2[n]$ of $y[n]$ from the first half-period $y_1[n]$ to obtain $r_a[n]$.

$$\begin{aligned} r_a[n] &= (y_1[n] - y_2[n]) \otimes h[n] + z_1[n] + z_2[n] \\ &= (y_1[n] - y_2[n]) \otimes h[n] + z[n] \end{aligned} \tag{11}$$

where, $z_1[n]$ is the AWGN during $y_1[n]$ and $z_2[n]$ is the AWGN during $y_2[n]$ and $z[n] = z_1[n] + z_2[n]$ denotes the sum Gaussian noise which has the power σ_z^2. The second step is flipping the polarity of the -ve samples of $r_a[n]$ followed by a horizontal concatenation with the +ve samples of $r_a[n]$ to form a length N time-domain symbol $r_b[n]$.

$$r_b[n] = (-r_a^+[n] \parallel r_a^-[n]) \otimes h[n] + z[n] \tag{12}$$

where r_a^+ represents the +ve samples of $r_a[n]$, r_a^- represents the -ve samples of $r_a[n]$ and $(\parallel)$ denotes the concatenation operator. The last step to obtain the input signal to the FFT operation $r[n]$ is the summation of $y[n]$ and $r_b[n]$.

$$r[n] = (y[n] + r_b[n]) \otimes h[n] + z[n] + z[n] \tag{13}$$

where, $z[n] + z[n]$ denotes the sum Gaussian noise which has the power $2\sigma_z^2$. The noise power of the SEE-OFDM is doubled during the reconstruction of the signal before the FFT operation. In a single-path (conventional ACO-OFDM), since there is no reconstruction, the noise power is σ_z^2 (*i.e.*, half of the amount in SEE-OFDM). The equivalent SNR per received sample for two-paths SEE-OFDM is given by,

$$\text{SNR} = \frac{\sigma_x^2}{2\sigma_z^2} = 20 \log_{10} \frac{\sigma_x}{2\sigma_z} \tag{14}$$

where, σ_x^2 denotes the transmitted signal power.

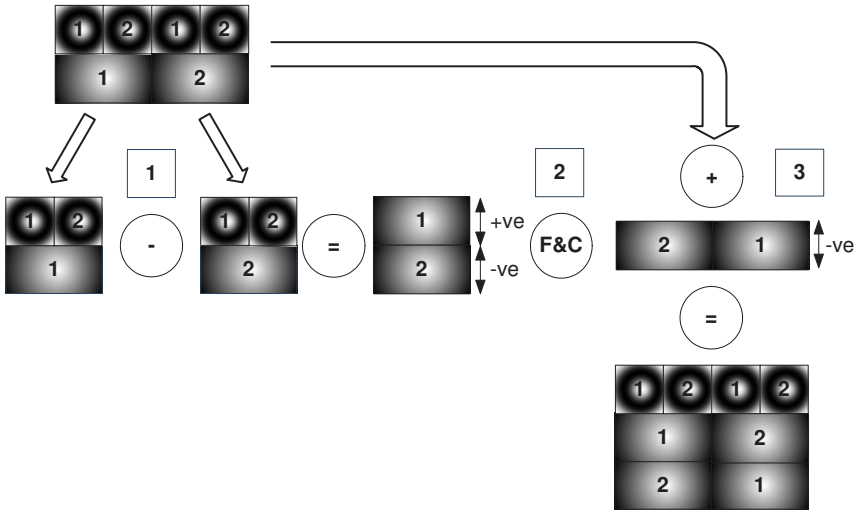

Figure 3: Two-paths SEE-OFDM reconstruction steps.

There is a possibility to include an additional path to realize a three-path SEE-OFDM system. The same procedure explained above for the two-paths SEE-OFDM is valid. Fig. 4 shows the signal modulating the LED and the reconstructed signal at the receiver before applying the FFT. The achieved data rate for such three-paths SEE-OFDM system is given by,

$$\begin{aligned} R_{\text{total}} &= R_{\text{path 1}} + R_{\text{path 2}} + R_{\text{path 3}} \\ &= \left(\frac{(N/4) + (N/8) + (N/16)}{N + N_{\text{CP}}}\right) B \log_2 M \end{aligned} \tag{15}$$

The equivalent SNR per received sample for three-paths SEE-OFDM is given by,

$$\text{SNR} = \frac{\sigma_x^2}{3\sigma_z^2} = 20 \log_{10} \frac{\sigma_x}{3\sigma_z} \tag{16}$$

The SNR from (Equ. (14) and Equ. (16)) can be plugged in the well-known formula for M-QAM bit-error rate (BER) performance [11]. Under this definition, the SNR penalty in the two-paths SEE-OFDM is 6dB when the noise variance is 2 times larger than the noise variance of the single-path SEE-OFDM. The SNR penalty in the three-paths SEE-OFDM is 10dB when the noise variance is 3 times larger than the noise variance of the single-path SEE-OFDM.

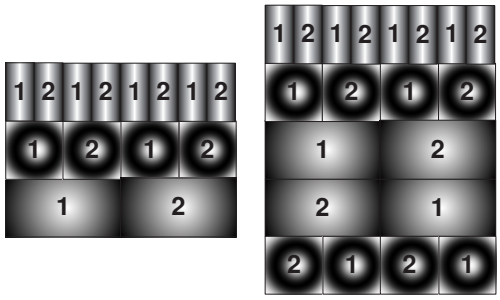

Figure 4: Three-paths SEE-OFDM signals.

Each LED has a minimum recommended forward current i_{LED} according to the data sheet, which is the onset of current flow and light emission. The LED outputs light that is linear with the drive current. However, thermal aspects causing a drop in the electrical-to-optical conversion efficiency must be considered. Hence, AC/pulsed currents must be adjusted according to the manufacturers data sheet to ensure that the LED chip does not overheat, in order to avoid degradation in output light or, in the worst case, total failure. The dynamic range of the optical source is determined by I_{L}, the minimum drive current (threshold or turn-on current) and I_{H}, the maximum allowed drive current [12]. Thus samples above I_{H} are clipped and the induced clipping noise is added to the AWGN to determine the effective noise/SNR. The LED model behavior can be described as follows:

$$i_{\text{LED}} = \begin{cases} I_{\text{H}} & \text{if } i_{\text{LED}} \geq I_{\text{H}} \\ i_{\text{LED}} & \text{if } i_{\text{LED}} < I_{\text{H}} \end{cases} \tag{17}$$

The clipping noise power, σ_c^2, reduces the effective SNR, SNR_{eff}, to,

$$\text{SNR}_{\text{eff}} = \frac{\sigma_{\text{x}}^2}{\sigma_{\text{z}}^2 + \sigma_{\text{c}}^2} \tag{18}$$

4 Simulation Results

For Monte Carlo simulations, the SEE-OFDM system is implemented using 16 subcarriers. For a fair comparison between single-path, two-paths and three-paths approaches, (1) the un-coded QAM constellations are set to insure a similar effective data rate and (2) the average power calculated over one time-domain OFDM symbol of length N is maintained equal. This average power per OFDM symbol is split across the signals of the different paths. Shot noise and thermal noise at the receiver are modeled as AWGN with noise power of -15dBm. A line-of-sight (LOS) configuration is assumed, thus no samples are considered for CP with $N_{\text{CP}} = 0$.

First, simulations are conducted to investigate the influence of adding additional paths on the PAPR of the signal modulating the LED. In Fig. 5, the cumulative distribution function (CDF) plots of the PAPR for the single-path, two-paths and three-paths approaches are depicted. Indeed, the two-paths approach has low PAPR as compared to the single-path for the same number of subcarriers. The 1.5dB reduction in PAPR is explained by the average power split across the two paths at a fixed average power per OFDM symbol. The PAPR of the three-paths is about 2.5dB and 1dB compared to the single-path and the two-paths, respectively. A low PAPR is desired due to the limiting dynamic range of LEDs.

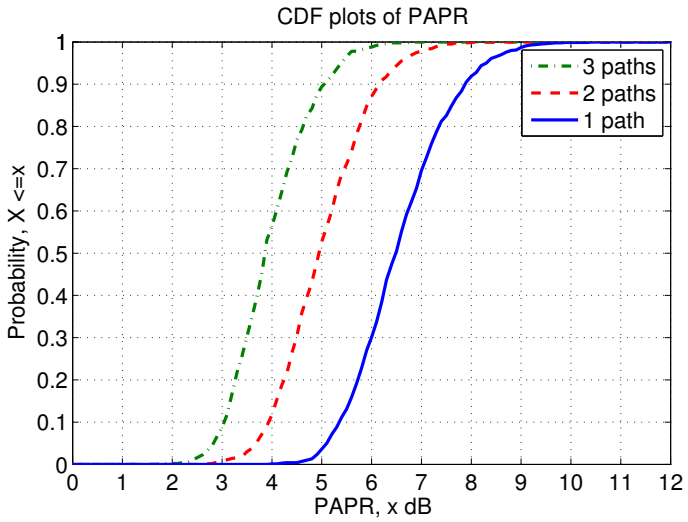

Figure 5: CDF plots of PAPR for $N = 16$.

Now the bit-error performance quantified by the BER as a function of SNR is discussed. As shown on Fig. 6, the simulated and analytical BER performance of the single-path and the two-paths are compared using a theoretical model and Monte Carlo simulations. The simulated electrical SNR range is from 10dB up to 46dB which is within the reported measured SNR values for indoor OWC systems. It is clearly confirmed that at the same effective data rate, the two-paths offer a superior BER performance at high-order QAM constellations. For a target BER of 10^{-3} (below the forward error correction (FEC) limit), single-path using 12-bits and two-paths using 8-bits per subcarrier, a 6dB SNR gain is obtained. For single-path using 9-bits and two-paths using 6-bits per subcarrier, about 3dB SNR gain is obtained. At low-order QAM constellations, the BER performance curves of both approaches are almost overlapping. Such overlapping indicates the effectiveness of the two-paths approach across the whole range of SNR values. There is good

agreement between the presented model and the conducted simulations.

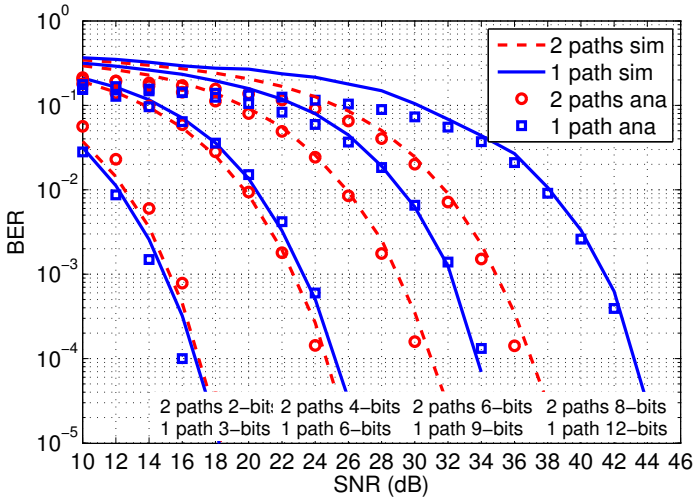

Figure 6: BER vs. SNR for the single-path and two-paths.

Simulations are also conducted to validate the effectiveness of adding a third path. At the same effective data rate, Fig. 7 shows the BER as a function of SNR for the single-path, two-paths and three-paths approaches using 9-bits, 6-bits and 5-bits per subcarrier, respectively. The three-paths approach shows a better BER compared to the single-path approach of around 1dB at 10^{-3} BER. However, the two-paths approach is still dominating the BER performance with about 1dB gain in SNR compared to the three-paths approach. The reason is explained by the increase in the noise power; a 10dB SNR penalty relative to the single-path approach after the reconstruction process at the receiver.

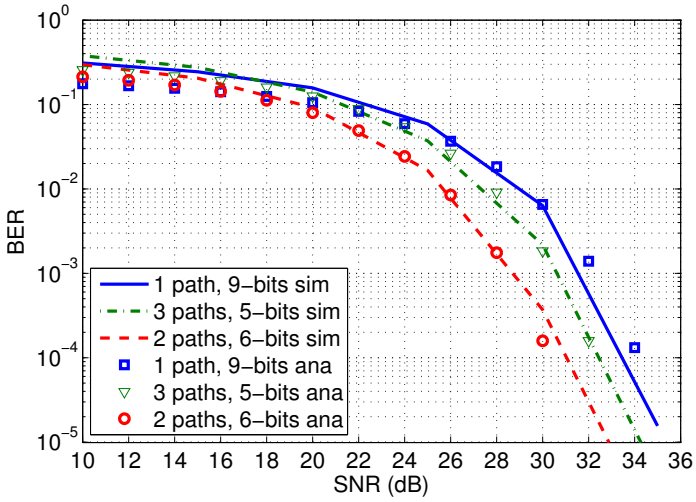

Figure 7: BER vs. SNR for the three approaches.

Finally, and at a fixed dynamic range of operation, the BER performance of the three approaches is investigated. We assume I_{L} = 0A and I_{H} = 0.5A, thus samples correspond to values above

0.5A are clipped and the induced clipping noise is added to the -15dBm AWGN to determine SNR_{eff}. As shown in Fig. 8, starting 10dB SNR, the BER is improved with the increase of the average signal power. Here the the signal power grows larger than the effective noise power. With a further increase, SNR_{eff} starts to decrease at certain amplitudes based on the PAPR of the individual approaches and consequently the BER starts to increase. Moreover, the effective noise power increases relative to the increase in the OFDM signal power. This is a trend that is valid for all approaches and the turning point is at 28dB, 29dB and 30dB for the single-path, two-paths and three-paths approaches using 9-bits, 6-bits and 5-bits per subcarrier, respectively. At the considered -15dBm AWGN, only the two-paths and the three-paths achieve BER below the FEC limit. The behavior of the rising BER curves confirm the lowest PAPR offered by the three-paths approach compared to the single-path and the two-paths approaches.

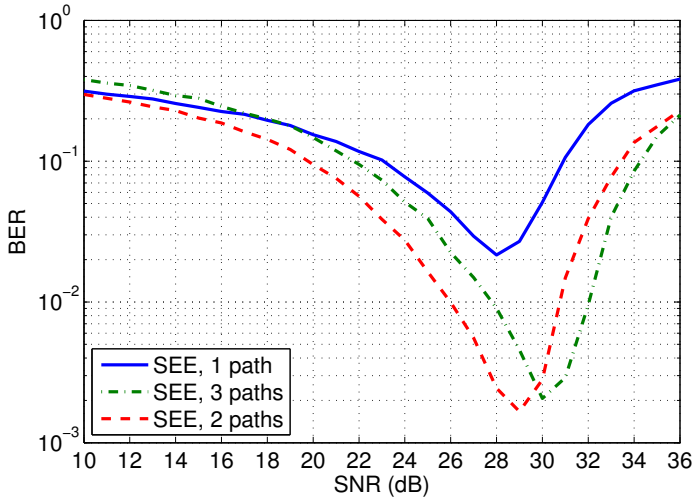

Figure 8: BER vs. SNR under dynamic range constraints.

5 Conclusion

The proposed SEE-OFDM is analyzed in the context of optical IM/DD transmission. While eliminating any DC bias level, the spectral efficiency is increased by about 90%, up to 6dB gain in SNR is demonstrated and PAPR is reduced by 2.5dB in comparison to the well-known unipolar ACO-OFDM. The receiver enables easy recovery of the transmitted symbols without any form of interference estimation and cancelation. A BER lower than FEC limit is maintained while maximizing data rate under a narrow dynamic range of operation. These features definitely make the SEE-OFDM very attractive.

References

[1] *More Than 50 Billion Connected Devices*, White Paper, (ERICSSON, 2013).

[2] Cisco Visual Networking Index, *Global Mobile Data Traffic Forecast Update, 2012-2017*, White Paper, (CISCO, 2013).

[3] J. G. Andrews, H. Claussen, M. Dohler, S. Rangan, M. C. Reed, "Femtocells: Past, Present, and Future," IEEE J. Sel. Areas Commun., **30** (3), 497–508 (2012).

[4] *Visible light communication (VLC) - a potential solution to the global wireless spectrum shortage*, Technical Report, (GBI Research, 2011).

[5] M. B. Rahaim, A. M. Vegni, and T. D. C. Little, "A hybrid radio frequency and broadcast visible light communication system," in GC Wkshps, 792–796, (IEEE, 2011).

[6] H. Elgala, R. Mesleh, and H. Haas, "Indoor optical wireless communication: potential and state-of-the-art," Communications Magazine, IEEE **49**(9), 56–62 (2011).

[7] R. Mesleh, H. Elgala, and H. Haas, "On the Performance of Different OFDM Based Optical Wireless Communication Systems," Optical Communications and Networking," Lightwave Technology, IEEE/OSA **3** (8), 620–628 (2011).

[8] R. Mesleh, H. Elgala, and H. Haas, "n overview of indoor OFDM/DMT optical wireless communication systems," in CSNDSP, 566–570, (IEEE, 2010).

[9] J. Armstrong and B. J. Schmidt, "Comparison of asymmetrically clipped optical OFDM and DC-biased optical OFDM in AWGN," Communications Letters, IEEE **12**(5), 343–345 (2008).

[10] N. Fernando, Y. Hong, and E. Viterbo, "Flip-OFDM for optical wireless communications," in ITW, 5–9, (IEEE, 2011).

[11] J. G. Proakis, *Digital Communications* (McGraw-Hill Science/Engineering/Math, 2000).

[12] H. Elgala, R. Mesleh, and H. Haas, "Modeling for predistortion of LEDs in optical wireless transmission using OFDM," in HIS, 12–14, (IEEE, 2009).